Control and Intelligent Systems, Vol. 38, No. 4, 2010

REDUCED-ORDER OBSERVER CONTROL FOR TWO-AREA LFC SYSTEM AFTER DEREGULATION

Elyas Rakhshani* and Javad Sadeh**

Abstract

In this paper, a reduced-order state observer with a practical point of view for load frequency control (LFC) problem in a deregulated power system is proposed. In the practical environment, there is limited access to all state variables of system and measuring all of them is usually impossible. So when the available sensors are less than the number of states or when it may be undesirable, expensive or impossible to measure directly all of the states, a reduced-order state observer can be applied as proposed in this paper. The proposed strategy is tested on a two-area power system and compared with the optimal full-state feedback method by using computer simulation. The results show that the proposed method improves the dynamic response of system and provides a control system that satisfies the LFC requirements.

Key Words

Automatic generation control, load frequency control, deregulated power system, reduced-order observer, optimal full-state feedback

Nomenclature

ACE	area control error
AGC	automatic generation control
APF	area participation factor
cpf	contract participation factor
DISCO	distribution company
DPM	disco participation matrix
GENCO	generation company
ISO	independent system operator
LFC	load frequency control
TRANSCO	transmission company
VIU	vertically integrated utility
B	frequency bias
R	droop characteristic
K_P	power system equivalent gain
T_P	power system equivalent time constant
T_G	governor time constant
T_T	turbine time constant
ΔP_L	contracted demand of DISCO
ΔP_M	power generation of GENCO
T_{12}	tie-line synchronizing coefficient between areas

* Islamic Azad University, Gonabad Branch, Gonabad, Iran; e-mail: elyas.rakhshani@gmail.com

** Electrical Engineering Department, Faculty of Engineering, Ferdowsi University of Mashhad, Mashhad, Iran; e-mail: sadeh@um.ac.ir

Recommended by Prof. M. Saif
(10.2316/Journal.201.2010.4.201-2110)

1. Introduction

In the last decade, a worldwide trend towards restructuring and deregulating of the power industry is seen. It was to develop effectiveness in the operation of the system by means of restructuring the industry and prepare a private competition. That is a worldwide trend and similar basic changes in other industries, i.e. in the airline transportation and telecommunications industries have appeared. It means that the transmission, generation, and distribution systems must now adapt to a new set of policies ordered by open markets. The electric power utilities in many countries have been, or are being, restructured.

Automatic Generation Control is a way of automatically controlling the outputs of power generating units to perform economic dispatch, and keep system frequency and power flows over tie-lines at preferred levels. AGC is performed at energy control centers or energy coordination centers using energy management systems. It was necessary to improve the AGC system for adjustment to the market environment with numerous kinds of the bidding strategies. Its fundamental theory is greatly discussed and well-known [1–5]. With the deregulation of electric markets, automatic generation control necessities should be expanded to comprise the market contracts and planning functions. So AGC is one of the ancillary services conventionally related with the activity of electricity generation and the further modifications were prepared at the AGC controller to meet the requirements of deregulation processes. Thus, the AGC system follows the temporary active power imbalance, detects and corrects it and

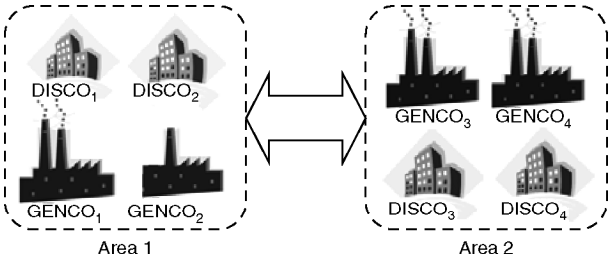

Figure 1. The configuration of the power system.

transfers an adequate amount of the balance energy according to the market operating system.

During the last decade, several proposed AGC scenarios attempted to adapt traditional AGC schemes for changing environment in the power systems under deregulation [6–13]. Some of these studies modified the conventional AGC system to take into account the effect of bilateral contracts on the dynamics [6, 7] or to improve the dynamical transient response of system under competitive conditions [8–13]. The conventional control strategy for the load frequency control (LFC) problem is to take the integral of the area control error (ACE) as the control signal. An integral controller provides zero steady-state deviation, but it exhibits poor dynamic performance. To improve the transient response, various control strategies, such as linear feedback, optimal control and Kalman estimator method, have been proposed [8, 9]. There have been continuing efforts in designing LFC with better performance using intelligence algorithms or robust methods [10–13]. Despite the proper dynamical responses, some of them had complex and high-order dynamical controllers.

In this paper, the dynamical response of the AGC problem in the competitive environment improved with a functional sight. In the real world, there is limited access to all state variables of system and little possibility of measuring all of them. Therefore, when the available sensors are less than the number of states or when it may be undesirable, expensive, or impossible to measure directly all of the states, a reduced-order state observer can be applied as proposed in this paper. The proposed method is evaluated on a two-area power system under contracted scenarios. The results of the proposed controller are compared with the optimal full-state feedback control by means of computer simulations. Results show that the proposed method improves the dynamic response of system and provides a control system that satisfies the LFC requirements.

2. Restructured Power System for AGC with Two Areas

In a competitive environment, vertically integrated utilities (VIU) no longer exist, instead there are three kind of entities such as GENCOs, DISCOs and transmission companies (TRANSCOs). However, the common AGC goals, i.e. restoring the frequency and the net interchanges to their preferred values for each control area, still remain [14]. The power system is assumed to comprise two areas and each area includes two GENCOs and also two DISCOs as shown in Fig. 1 and the block diagram of the generalized LFC scheme for a two area deregulated power system is shown in Fig. 2.

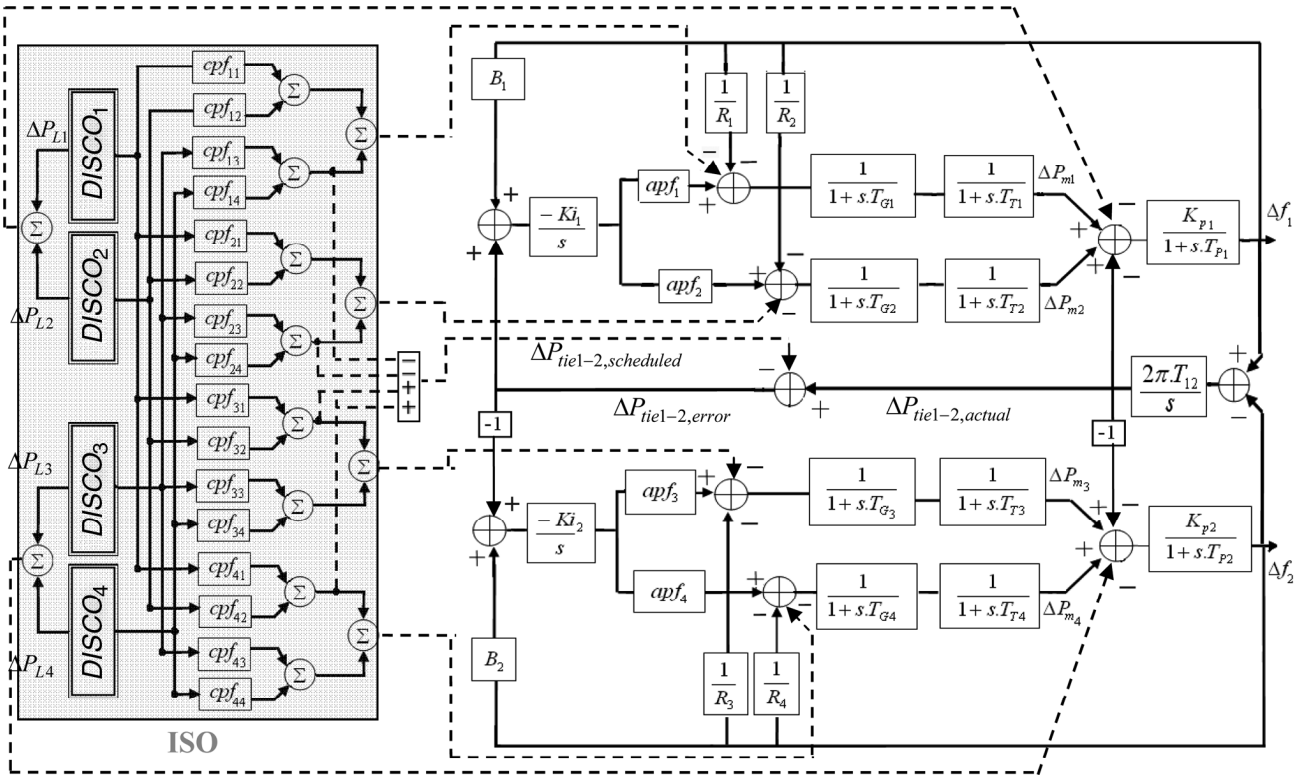

Figure 2. Modified LFC system in a deregulated environment.

In the deregulated power system, GENCOs may or may not participate in the AGC task. On the other hand, DISCOs have the liberty to contract with any available GENCO in their own or other areas. Thus, there can be various combinations of the possible contracted scenarios between DISCOs and GENCOs [14].

So, a DISCO can contract individually with any GENCO for energy and these transactions are made under the supervision of ISO. To make the visualization of contracts easier, the concept of a "DISCO participation matrix" (DPM) is used [7]; essentially, DPM gives the participation of a DISCO in contract with a GENCO. In DPM, the number of rows has to be equal to the number of GENCOs and the number of columns has to be equal to the number of DISCOs in the system. Any entry of this matrix is a fraction of total load power contracted by a DISCO with a GENCO. So, summation of entries in each column of DPM which is related to DISCO_j is one and $\sum_i cpf_{ij} = 1$. The corresponding DPM for the studied power system have two areas and each of them includes two DISCOs and two GENCOs, which is given as follows [14]:

$$\text{DPM} = \begin{array}{c} \\ 1 \\ 2 \\ 3 \\ 4 \end{array} \begin{array}{c} \begin{array}{cccc} \text{D} & \text{I} & \text{S} & \text{C} & \text{O} \end{array} \\ \left(\begin{array}{cc|cc} 1 & 2 & 3 & 4 \\ cpf_{11} & cpf_{12} & cpf_{13} & cpf_{14} \\ cpf_{21} & cpf_{22} & cpf_{23} & cpf_{24} \\ \hline cpf_{31} & cpf_{32} & cpf_{33} & cpf_{34} \\ cpf_{41} & cpf_{42} & cpf_{43} & cpf_{44} \end{array}\right) \end{array} \begin{array}{c} \\ \text{G} \\ \text{E} \\ \text{N} \\ \text{C} \\ \text{O} \end{array}$$

where *cpf* represents "contract participation factor" which include information that determines which GENCO has the responsibility of following a load demanded by each DISCO. The actual and scheduled steady-state power flows on the tie-line are given as:

$$\Delta P_{tie1\text{–}2,scheduled} = \sum_{i=1}^{2}\sum_{j=3}^{4} cpf_{ij}\Delta P_{Lj} - \sum_{i=3}^{4}\sum_{j=1}^{2} cpf_{ij}\Delta P_{Lj} \quad (1)$$

$$\Delta P_{tie1\text{–}2,actual} = (2\pi \cdot T_{12}/s) \cdot (\Delta f_1 - \Delta f_2) \quad (2)$$

And at any given time, the tie-line power error $\Delta P_{tie1-2,error}$ is defined as:

$$\Delta P_{tie1\text{–}2,error} = \Delta P_{tie1\text{–}2,actual} - \Delta P_{tie1\text{–}2,scheduled} \quad (3)$$

This error signal is used to generate the respective ACE signals as in the traditional scenario [7]:

$$ACE_1 = B_1\Delta f_1 + \Delta P_{tie1-2,error} \quad (4)$$

$$ACE_2 = B_2\Delta f_2 + \Delta P_{tie2-1,error} \quad (5)$$

where B_1, B_2 are the frequency bias of areas 1 and 2, respectively. The closed-loop system in Fig. 2 is characterized in state space form as:

$$\dot{x} = A \cdot x + B \cdot u \quad (6)$$

$$y = C \cdot x \quad (7)$$

A fully controllable and observable dynamic model for a two-area power system is proposed, where x is the state vector and u is the vector of power demands of the DISCOs [15].

$$u = [\ \Delta P_{L1} \quad \Delta P_{L2} \quad \Delta P_{L3} \quad \Delta P_{L4}\ ]^T$$

$$x = [\ \Delta f_1 \quad \Delta f_2 \quad \Delta P_{m1} \quad \Delta P_{m2} \quad \Delta P_{m3} \quad \Delta P_{m4} \quad \int ACE_1 \quad \int ACE_2 \quad \Delta P_{tie1\text{–}2,actual}\ ]^T$$

where ΔP_L is contracted demand of DISCOs and the deviation of frequency, turbine output and tie-line power flow within each control area are measurable outputs, other states are not measurable and should be estimated by applying reduced-order observer. The dashed lines in Fig. 2 show the demand signals based on the possible contracts between GENCOs and DISCOs. They include information that determines which GENCO has the responsibility of following a load demanded by each DISCO. These new information signals were absent in the traditional LFC scheme. As there are many GENCOs in each area, the ACE signal has to be distributed among them due to their ACE participation factor in LFC and $\sum_j apf_{ji} = 1$.

3. Controller Design

In this paper, to improve the dynamical response of system pragmatically, reduced-order observer method is proposed, but to have a complete research, optimal full-state feedback control is designed and the results are compared. When feedback control law is $u = -K \cdot x$, and some of the state variables in vector x are not measurable, using the observer to estimate the unmeasurable states is an option [16, 17]. A full-order observer estimates all the states in a system, regardless whether they are measurable or not but when some of the state variables are measurable using a reduced-order observer is so better.

3.1 Reduced-Order Observer Controller

For the system defined by (6) and (7), feedback control law is:

$$u = -K \cdot y \quad (8)$$

In practical environments, only some of the state variables are measurable. These are defined as output variables such as:

$$y_{p\times 1} = C_{p\times n} \cdot x_{n\times 1}, \quad p < n \quad (9)$$

The interesting case is when we have less sensors available (p) than the number of states (n), $p < n$.

Suppose we can measure some of the state variables contained in x, and the state vector x is partitioned into two sets,

x_1: variables that can be measured directly,

x_2: variables that cannot be measured directly.

$$\begin{cases} \dot{x}_1 = A_{11} \cdot x_1 + A_{12} \cdot x_2 + B_1 \cdot u \\ \dot{x}_2 = A_{21} \cdot x_1 + A_{22} \cdot x_2 + B_2 \cdot u \end{cases} \tag{10}$$

and the observation equation is:

$$y = C_1 \cdot x_1 \tag{11}$$

where C_1 is square and non-singular matrix. The full-order observer for the states is then:

$$\begin{cases} \dot{\hat{x}}_1 = A_{11} \cdot \hat{x}_1 + A_{12} \cdot \hat{x}_2 + B_1 \cdot u + L_1 \cdot (y - C_1 \cdot \hat{x}_1) \\ \dot{\hat{x}}_2 = A_{21} \cdot \hat{x}_1 + A_{22} \cdot \hat{x}_2 + B_2 \cdot u + L_2 \cdot (y - C_1 \cdot \hat{x}_1) \end{cases} \tag{12}$$

But we do not need to solve first observer equation for x_1 because these states can be solved directly using (11):

$$\hat{x}_1 = x_1 = C_1^{-1} \cdot y \tag{13}$$

In this case, the observer for those states that cannot be measured directly is designed as follows:

$$\dot{\hat{x}}_2 = A_{21} \cdot C_1^{-1} \cdot y + A_{22} \cdot \hat{x}_2 + B_2 \cdot u \tag{14}$$

The block diagram of this reduced-order observer is shown in Fig. 3. This is a dynamic system of the same order as the number of state variables that cannot be measured directly. The dynamic behaviour of this reduced-order observer is governed by the eigenvalues of A_{22}, this is a matrix that the designer has no control on it. As there is no assurance that the eigenvalues of A_{22} are suitable, we need a more general system for the reconstruction of x_2. We take:

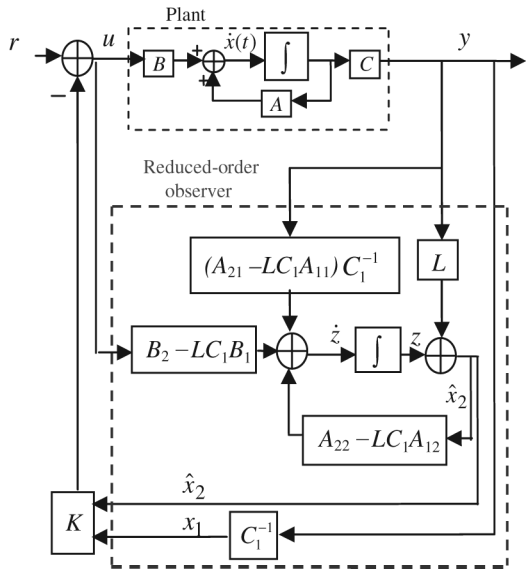

Figure 3. Block diagram of reduced-order observer.

$$\hat{x}_2 = L \cdot y + z \tag{15}$$

where:

$$\dot{z} = F \cdot z + G \cdot y + H \cdot u \tag{16}$$

Define the estimation error as follows:

$$e = x - \hat{x} = \begin{bmatrix} x_1 - \hat{x}_1 \\ x_2 - \hat{x}_2 \end{bmatrix} = \begin{bmatrix} e_1 \\ e_2 \end{bmatrix} = \begin{bmatrix} 0 \\ e_2 \end{bmatrix} \tag{17}$$

and we get:

$$\begin{aligned} \dot{e}_2 &= \dot{x}_2 - \dot{\hat{x}}_2 = A_{21} \cdot x_1 + A_{22} \cdot x_2 + B_2 \cdot u - L \cdot \dot{y} - \dot{z} \\ &= A_{21} \cdot x_1 + A_{22} \cdot x_2 + B_2 \cdot u - LC_1 \cdot \dot{x}_1 - F \cdot z \\ &\quad - G \cdot y - H \cdot u \\ &= A_{21} \cdot x_1 + A_{22} \cdot x_2 + B_2 \cdot u - LC_1(A_{11} \cdot x_1 + \\ &\quad A_{12} \cdot x_2 + B_1 \cdot u) - F(\hat{x}_2 - L \cdot y) - G \cdot y - H \cdot u \end{aligned} \tag{18}$$

As:

$$\hat{x}_2 - L \cdot y = x_2 - e_2 - L \cdot y = x_2 - e_2 - LC_1 \cdot x_1 \tag{19}$$

We have:

$$\begin{aligned} \dot{e}_2 &= Fe_2 + (A_{21} - LC_1A_{11} - GC_1 + FLC_1)x_1 \\ &\quad + (A_{22} - LC_1A_{12} - F) \cdot x_2 + (B_2 - LC_1B_1 - H)u \end{aligned} \tag{20}$$

In order for the error to be independent of x_1, x_2, and u, the matrices multiplying x_1, x_2, and u must vanish:

$$\begin{cases} F = A_{22} - LC_1A_{12} \\ H = B_2 - LC_1B_1 \\ G = (A_{21} - LC_1A_{11})C_1^{-1} + FL \end{cases} \tag{21}$$

Then:

$$\dot{e}_2 = F \cdot e_2 \tag{22}$$

For stability of the observer dynamic system, the eigenvalues of F must lie in the left-hand side of s plane. Therefore, we see that the problem of reduced-order observer is similar to the full-order observer with $(A_{22} - LC_1A_{12})$ playing the role of $(A - LC)$.

In this paper, for application of this reduced-order state observer to the LFC problem, x_1 and x_2 are specified and as shown in Fig. 4, a reduced-order observer estimates unmeasurable states such as $\int \mathrm{ACE}_1$ and $\int \mathrm{ACE}_2$. More

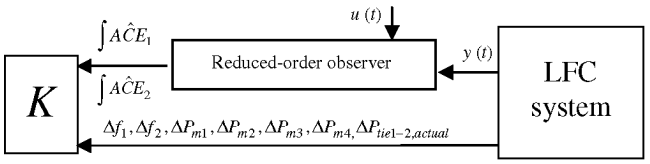

Figure 4. Schematic diagram of applied reduced-order observer for LFC.

details about this implementation are presented at the end of Section 4.

$$x_1 = [\Delta f_1 \quad \Delta f_2 \quad \Delta P_{m1} \quad \Delta P_{m2} \quad \Delta P_{m3} \quad \Delta P_{m4} \quad \Delta P_{tie1-2,actual}]^T$$
$$x_2 = [\int ACE_1 \quad \int ACE_2]^T$$

4. Simulation Results

In this section, to illustrate the performance of the proposed controller against load variations, simulations are performed for one scenario of possible contracts under various operating conditions and large load demands. In this scenario, the performance of the proposed controller is compared with optimal full-state feedback controller. The simulations are performed with MATLAB platform and the power system parameters are given in Tables 2 and 3.

Based on the information given in Section 3, the system can be expressed in the following partitioned form:

$$A = \left[\begin{array}{c|c} A_{11_{(n-r)\times(n-r)}} & A_{12_{(n-r)\times r}} \\ A_{21_{r\times(n-r)}} & A_{22_{r\times r}} \end{array}\right]_{n\times n}$$

$$B = \left[\begin{array}{c} B_{1_{(n-r)\times d}} \\ \hline B_{2_{r\times d}} \end{array}\right]_{n\times d}$$

where:
$n = 9$ is the number of variables of system;
$r = 2$ is the number of unmeasurable variables;
$d = 4$ is the number of inputs of system.

Also according to the design procedure discussed in previous section, the state space values of these matrices are obtained as follows:

$$A_{11} = \begin{bmatrix} -0.05 & 0 & 5.1 & 5.1 & 0 & 0 & -5.10 \\ 0 & -0.04 & 0 & 0 & 4.08 & 4.08 & 4.08 \\ -0.1745 & 0 & -2.6316 & 0 & 0 & 0 & 0 \\ -0.1675 & 0 & 0 & -2.6316 & 0 & 0 & 0 \\ 0 & -0.1768 & 0 & 0 & -2.7778 & 0 & 0 \\ 0 & -0.1511 & 0 & 0 & 0 & -2.5641 & 0 \\ 0.0390 & -0.390 & 0 & 0 & 0 & 0 & 0 \end{bmatrix}$$

$$A_{12} = \begin{bmatrix} 0 & 0 \\ 0 & 0 \\ -1.3816 & 0 \\ -0.4605 & 0 \\ 0 & -0.9722 \\ 0 & -0.8974 \\ 0 & 0 \end{bmatrix}, \quad A_{21} = \begin{bmatrix} 0.0676 & 0 & 0 & 0 & 0 & 0 & 1.00 \\ 0 & 0.0631 & 0 & 0 & 0 & 0 & -1.0 \end{bmatrix}, \quad A_{22} = \begin{bmatrix} 0 & 0 \\ 0 & 0 \end{bmatrix}$$

$$B_1 = \begin{bmatrix} -5.1000 & -5.1000 & 0 & 0 \\ 0 & 0 & -4.0800 & -4.0800 \\ 1.3158 & 0.6579 & 0 & 0.7895 \\ 0 & 0 & 0 & 0 \\ 0 & 1.3889 & 2.7778 & 1.9444 \\ 1.2821 & 0.6410 & 0 & 0 \\ 0 & 0 & 0 & 0 \end{bmatrix}, \quad B_2 = \begin{bmatrix} 0.500 & 0.750 & 0 & -0.300 \\ -0.500 & -0.750 & 0 & 0.300 \end{bmatrix}$$

Note that the observer has to be slightly faster than the process, so the error becomes zero after a short time period [16]. This behaviour is obtained by placing the poles of the matrix $(A_{22} - LC_1A_{12})$ to the left of the poles of the uncontrolled system.

The observer gains, entries of Matrix L, have a direct effect on observer responses. By properly selecting the observer gains, one can arrange the observer eigenvalues in such a way that the system dynamic response becomes stable. More proofs about this fact can be found in [16].

The observer gain is chosen in a manner that the observer poles are placed at the desired locations, but it is important to note that the observer gains are usually small to enhance the observer robustness against noise [18]. So a set of matrix equations presented by (21) must be solved simultaneously using an iteration algorithm or LMI approach [18]. This calculated observer gain is presented as below:

$$L = \begin{bmatrix} 1.6712 & -2.1985 & -1.8106 & 1.8344 & 1.3519 & -2.3150 & -0.8492 \\ -1.6778 & 1.3643 & 0.2292 & 0.3247 & -2.9504 & 1.0938 & 1.4516 \end{bmatrix}$$

Then the eigenvalues of $(A_{22} - LC_1A_{12})$ are $\{-1.7717 + 0.5852\,i, -1.7717 - 0.5852\,i\}$ and dynamic of designed observer is stable:

$$F = A_{22} - L \cdot C_1 \cdot A_{12} = \begin{bmatrix} -1.6567 & -0.7632 \\ 0.4661 & -1.8868 \end{bmatrix}$$

4.1 Scenario: Transaction Based on Free Contracts

In this scenario, DISCOs have the freedom to have a contract with any GENCO in their or other areas. So in this scenario, all the DISCOs contract with the GENCOs based on following DPM:

$$\text{DPM} = \begin{bmatrix} 0.5 & 0.25 & 0 & 0.3 \\ 0 & 0 & 0 & 0 \\ 0 & 0.5 & 1 & 0.7 \\ 0.5 & 0.25 & 0 & 0 \end{bmatrix}$$

Second row of the above DPM shows that GENCO_2 does not have any contract with other DISCOs. So, it is assumed that each DISCO demands 0.1 pu MW total power from other GENCOs as defined by entries in DPM and these GENCOs participates in AGC as defined by the following *apf*s:

$$apf_1 = 0.75, \quad apf_2 = 1 - apf_1 = 0.25$$
$$apf_3 = 0.5, \quad apf_4 = 1 - apf_3 = 0.5$$

If uncontracted loads are absent, ACE participation factors affect only the transient behaviour of the system, not steady-state behaviour.

As shown in Fig. 5, in the steady state, any GENCO generation must match the demand of the DISCOs in contract with it, as expressed as follows:

$$\Delta P_{mi} = \sum\nolimits_j cpf_{ij} \Delta P_{Lj} \tag{23}$$

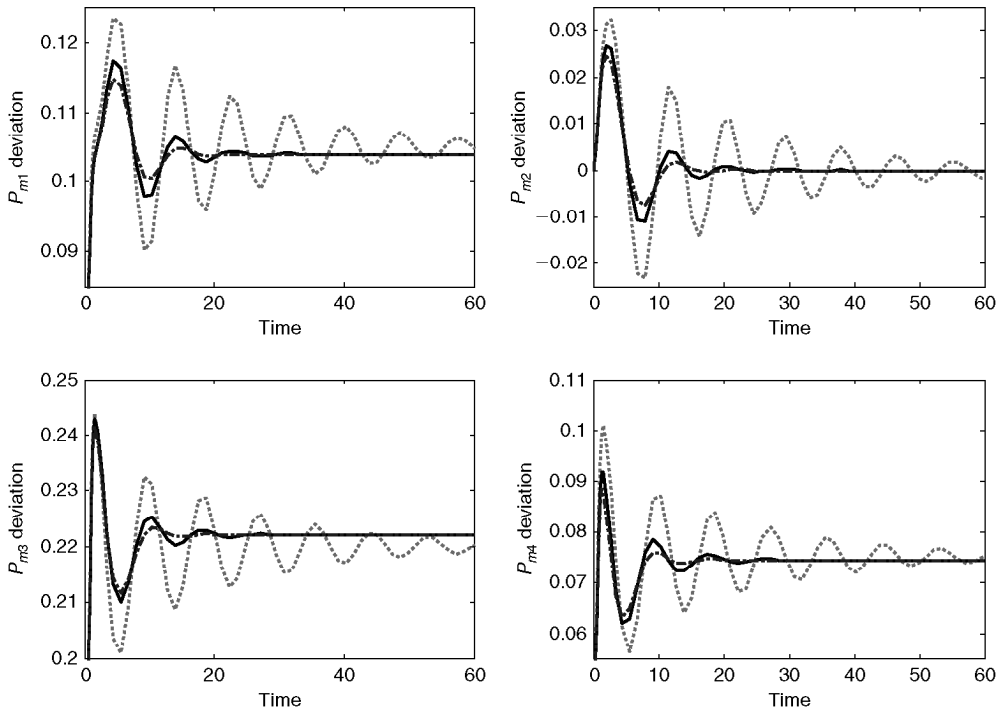

Figure 5. GENCOs power change (pu MW): solid (with reduced-order observer control), dotted (without controller), dot-dashed (optimal full-state feedback).

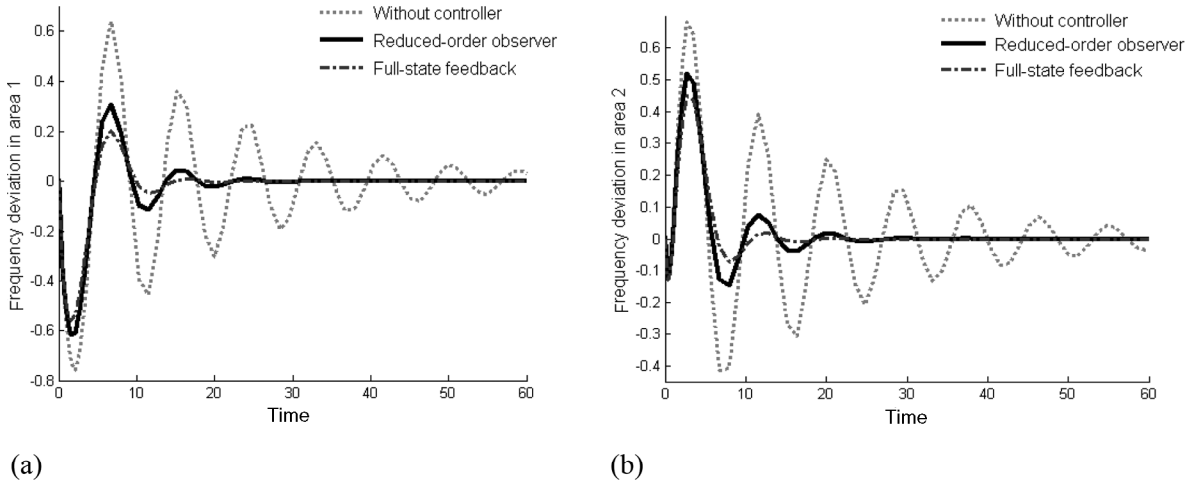

Figure 6. (a) Frequency deviation in area 1 (rad/s) and (b) frequency deviation in area 2 (rad/s): dotted (without controller), solid (reduced-order observer control), dot-dashed (optimal full-state feedback).

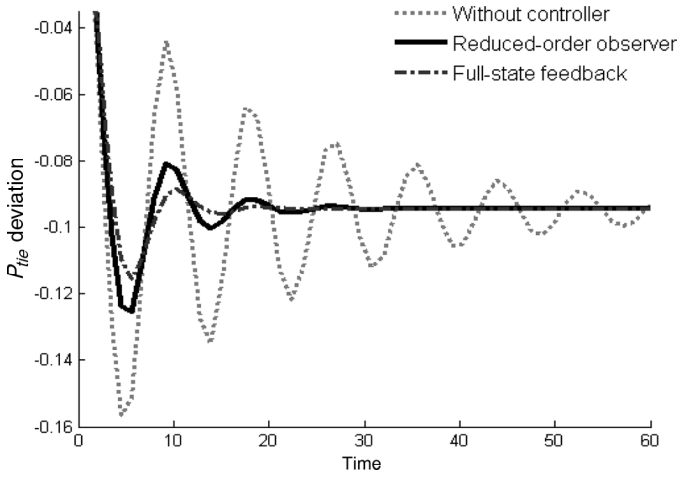

Figure 7. Deviation of tie line power flow (pu MW): dotted (without controller), solid (reduced-order observer control), dot-dashed (optimal full-state feedback).

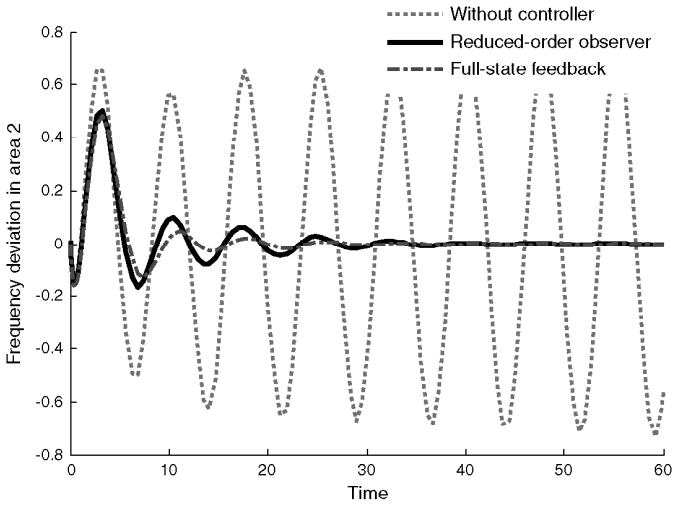

Figure 8. The frequency deviation in area 2 (rad/s): dotted (without controller), solid (reduced-order observer control), dot-dashed (optimal full-state feedback).

So for this scenario, we have:

$$\Delta P_{m1} = 0.5(0.1) + 0.25(0.1) + 0 + 0.3(0.1) = 0.105\,\text{pu MW}$$

$$\Delta P_{m2} = 0.0\,\text{pu MW}$$

$$\Delta P_{m3} = 0.22\,\text{pu MW}$$

$$\Delta P_{m4} = 0.075\,\text{pu MW}$$

The results for this case are given in Figs. 5–7. Using the proposed method, the frequency deviation of each area and the tie-line power have a good dynamic response in comparing with initial system without controller. The results of frequency deviations and tie-line power flow are shown in Figs. 6 and 7, respectively. These figures also show comparison between the performance of the proposed controller and the optimal full-state feedback.

The off-diagonal blocks of the DPM correspond to the contract of a DISCO in one area with a GENCO in another area. As shown in Fig. 7, the tie-line power flow properly converges to the specified value of (1) in the steady state, i.e., $\Delta P_{tie1-2,scheduled} = -0.095\,\text{pu MW}$.

4.2 Additional Property of the Proposed Method on Trajectory Sensitivity

In this section, to examine the effectiveness of the proposed method on reduction of trajectory sensitivity to plant-parameter variations, another case is simulated. In this case, previous scenario in Section 4.1 is simulated with 25% increase in system parameters, i.e., GENCOs parameters and 25% increase in demanded load by area 2. The frequency deviation of second area, with 25% increase in system parameters, is depicted in Fig. 8. It is observed that, by using the reduced-order observer method, the oscillations are damped out in around 30 s, whereas the

Table 1
Eigenvalues of the System

Modes	System without Controller	Full-State Feedback	Controller with a Reduced-Order Observer
Δf_1	$0.0029 + 0.8341i$	$-0.1853 + 0.2031i$	$-0.1597 + 0.8161\,i$
Δf_2	$0.0029 - 0.8341i$	$-0.1613 - 0.1140\,i$	$-0.1597 - 0.8161\,i$
ΔP_{m_1}	$-0.2019 + 0.6056i$	$-0.2360 + 0.01\,i$	$-0.2136 + 0.6101\,i$
ΔP_{m_2}	$-0.2019 - 0.6056i$	$-0.2211 - 0.6101\,i$	$-0.2136 - 0.6101\,i$
ΔP_{m_3}	-0.4758	-0.4506	-0.4475
ΔP_{m_4}	-1.6640	-1.7301	-1.7273
$\int ACE_1$	-1.9190	-2.1024	-2.5102
$\int ACE_2$	-2.1849	-2.4678	-2.4431
ΔP_{tie}	-2.2316	-2.2573	-2.1820

initial system is unstable. Table 1 shows the eigenvalues of the power system for this simulated case described in Section 2. It can be seen that two of the eigenvalues are on the right-hand side of s-plane, which means that without any control, the system is unstable.

5. Conclusion

In this paper, one of the most useful functions of a local reduced-order state observer for LFC problem in a deregulation power system is presented. In a practical environment, some of the state variables in the LFC system such as ACE or integration of ACE are not measurable. To solve this problem, a reduced-order state observer is proposed for estimation of these unmeasurable states. This controller allocates generating unit's output according to contracted scenarios. The performance of the proposed controller is evaluated through the simulation of two-area power system.

Analysis reveals that the proposed technique gives good results and usages of this method reduce the peak deviations of frequencies, tie-line power and time error. It can be concluded that the application of reduced-order observer to LFC of interconnected power system will be provided a practical sight. Also, this method can be used in a large AGC power system as a local estimator. The following conclusions can be drawn about the some advantages of proposed method:

1. The main advantage of this kind of reduced-order state observer is the capability of estimating unmeasurable states in a practical condition. In the case of LFC problem, there is a limitation for measuring some of states ($\int ACE_1$ and $\int ACE_2$), so this method can be used as a local controller for each area in a large power system.
2. Another important feature of the proposed strategy is that the separation property for design. In fact, based on the information presented in Sections 3 and 4, the design of controller and observer are independent. This behaviour is obtained by placing the poles of the matrix F to the left of the poles of the uncontrolled system. Based on the simulation results and the data in Table 1, it is clear that suitable allocating of observer poles result in improving the dynamic response of the system.

Appendix

A. Parameter values of the studied power system are given in Tables 2 and 3:

Table 2
GENCOs Parameters

GENCOs Parameters	Area 1		Area 2	
	$GENCO_1$	$GENCO_2$	$GENCO_3$	$GENCO_4$
T_T (s)	0.32	0.30	0.03	0.32
T_G (s)	0.06	0.08	0.06	0.07
R (Hz/pu)	2.4	2.5	2.5	2.7

Table 3
Control Area Parameters

Control Area Parameters	Area 1	Area 2
K_P(pu/Hz)	102	102
T_P(s)	20	25
B(pu/Hz)	0.425	0.396
T_{12}(pu/Hz)	0. 245	

References

[1] P. Kunder, *Power system stability and control* (USA: McGraw-Hill, 1994).

[2] H. Saadat, *Power system analysis* (USA: McGraw-Hill, 1999).

[3] O.I. Elgerd & C.E. Fosha, Optimum megawatt-frequency control of multi-area electric energy systems, *IEEE Transactions on Power Apparatus and Systems*, *89*(4), 1970, 556–563.

[4] N. Jaleeli, D.N. Ewart, & L.H. Fink, Understanding automatic generation control, *IEEE Transactions on Power Systems*, *7*(3), 1992, 1106–1112.

[5] A. Feliachi, Load frequency control using reduced order models and local observers, *Electrical Power and Energy Systems*, *7*(2), 1987, 72–75.

[6] J. Kumar, K.-H. Ng, & G. Sheble, AGC simulator for price-based operation part 1: A model, *IEEE Transactions on Power Systems*, *12*(2), 1997, 527–532.

[7] V. Donde, A. Pai, & I.A. Hiskens, Simulation and optimization in an AGC system after deregulation, *IEEE Transactions on Power Systems*, *16*(3), 2001, 481–489.

[8] F. Liu, Y.H. Song, J. Ma, S. Mei, & Q. Lu, Optimal load-frequency control in restructured power systems, *IEE Proceedings Generation, Transmission and Distribution*, *150*(1), 2003, 87–95.

[9] D. Rerkpreedapong & A. Feliachi, Decentralized load frequency control for load following services, *IEEE Power Engineering Society Winter Meeting*, *2*(1), 2002, 1252–1257.

[10] A. Demiroren & H.L. Zeynelgil, GA application to optimization of AGC in three-area power system after deregulation,*Electrical Power and Energy Systems*, *29*(3), 2007, 230–240.

[11] H. Bevrani, Y. Mitani, & K. Tsuji, Robust decentralized LFC design in a deregulated environment, *IEEE International Conf. on Electric Utility Deregulation, Restructuring and Power Technologies* (DRPT2004), 2004.

[12] H. Shayeghi, H.A. Shayanfar, & O.P. Malik, Robust decentralized neural networks based LFC in a deregulated power system, *Electric Power Systems Research*, *77*, 2007, 241–251.

[13] H. Shayeghi, H.A. Shayanfar, & O.P. Malik, Multi-stage fuzzy PID power system automatic generation controller in deregulated environments, *Energy Conversion and Management*, *47*(2), 2006, 2829–2845.

[14] E. Rakhshani & J. Sadeh, A reduced-order estimator with prescribed degree of stability for two-area LFC system in a deregulated environment, *IEEE/PES Power Systems Conference and Exposition*, Seattle, WA, 2009, 1–8.

[15] E. Rakhshani & J. Sadeh, Practical viewpoints on load frequency control problem in a deregulated power system, *Energy Conversion and Management*, *51*(6), 2010, 1148–1156.

[16] A.K. Sedigh, *Modern Control Systems* (University of Tehran Press, 2003).

[17] D.G. Luenberger, An introduction to observers, *IEEE Transactions on Automatic Control*, *16*(6), 1971, 596–602.

[18] K. Ma, F. He, & Y. Yao, Observer design for Lipschitz nonlinear system, *Control and Intelligent Systems*, *37*(2), 2009, 97–102.

Biographies

Elyas Rakhshani was born in Mashhad, Iran, in 1982. He received his B.Sc. degree in Power Engineering from Islamic Azad University of Iran, Birjand branch, Iran, in 2004 and M.Sc. degree in Control Engineering from Islamic Azad University of Iran, Gonabad branch, Iran, in 2008. His research interests are power system control, dynamics and operation, optimal control and neural computing.

Javad Sadeh was born in Mashhad, Iran, in 1968. He received his B.Sc. and M.Sc. degrees in Electrical Engineering from Ferdowsi University of Mashhad in 1990 and 1994, respectively, and his Ph.D. from Sharif University of Technology, Tehran, Iran, with the collaboration of the Electrical Engineering Laboratory of the National Polytechnic Institute of Grenoble (INPG), France, in 2000. Since then, he served as an assistant professor at the Ferdowsi University of Mashhad. His research interests are power system protection, electromagnetic transients in power system and restructuring.